Asian Journal of Chemistry; Vol. 37, No. 1 (2025), 145-148

ASIAN JOURNAL OF CHEMISTRY

https://doi.org/10.14233/ajchem.2025.32878

Synthesis and Characterization of Nanocellulose from Neem Sawdust as Biomass using Ionic Liquid

H.K. Pradeep[1,*], Dipti H. Patel[1], S. Sahana[2], N. Abhishek[2], H. Jeevan[2], V. Karthik[2], K.V. Tejasvini[2] and Divya V. Pattanashetty[2]

[1]Department of Pharmaceutics, Institute of Pharmaceutical Sciences, Faculty of Pharmacy, Parul University, P.O. Limda, Tal. Waghodia-391760, India
[2]Department of Pharmaceutics, GM Institute of Pharmaceutical Sciences and Research, Davanagere-577006, India

*Corresponding author: E-mail: pradeephkgmips@gmail.com

Received: 12 October 2024; *Accepted*: 9 December 2024; *Published online*: 31 December 2024; AJC-21861

The primary emphasis of the work was to synthesize and characterize nanocellulose from the ionic liquid method for potential biosensor application. The lignocellulosic material like neem sawdust was utilized to prepare cellulose by treating it with sodium hydroxide and sodium chlorite solution for the delignification and removal of hemicellulose. The obtained cellulose was employed to produce nanocellulose by treating it with ionic liquid. The obtained nanocellulose was characterized for FTIR, SEM, TGA, DTA and XRD techniques. The FTIR results suggest the successful conversion of cellulose to nanocellulose and highlights the functional groups. The β-glycosidic linkage at its peak is a main characteristic feature of the cellulose backbone which remains intact in each of the samples and was greatly preserved during nanocellulose processing. SEM analysis demonstrates that the nanocellulose has fibrils with a dense agglomeration of interconnected fibrils and also confirmed that nanocellulose has a higher surface area with high flexibility, good mechanical strength and good structural integrity. The XRD results indicate the increased crystallinity in the prepared nanocellulose. The TGA and DTA represent the limited thermal stability with major thermal degradation at a specified temperature range followed by the exothermic reaction. Nanocellulose synthesized through the ionic liquid method from lignocellulosic biomass and characterized which shows good structural and thermal properties.

Keywords: Nanocellulose, Neem sawdust, Crystalline structure, Ionic liquid.

INTRODUCTION

Lignocellulosic waste management is a global issue, especially tough for developing countries due to rapid population growth, immigration, urbanization and higher living standards [1]. According to a recent approach, worldwide lignocellulosic biomass production is around 181.5 billion tons per annum, 8.2 billion tons of which are used in different areas [2]. Uncontrolled waste dumping harms public and environmental health. Therefore, developing sustainable waste management systems is essential for the economic growth of these countries. This issue is critical for wood processing enterprises due to declining nearby industrial wood reserves. These enterprises generate significant waste, such as sawdust, bark and slabs, which are often burned or buried, leading to the environmental hazards. Practical experience shows that sawmills produce adequate sawdust regardless of the technology used. Adopting the use of this waste as an additional raw material is critical for the efficient utilization of timber resources [3].

Sawdust and wood shavings, the byproducts of woodworking processes such as sawing, planning, sanding and milling, hold immense potential as raw materials [4]. These lignocellulosic materials are not only abundant and affordable but also frequently pose disposal issues. Sawdust, for instance, is commonly used in farms and paper mills, with the surplus often being discharged untreated into the environment. However, with the appropriate methodology, these wastes can be converted into valuable resources, motivating wood processing companies and researchers to investigate creative ways for their effective exploitation [5]. The sawdust is often overlooked as a byproduct of wood processing and has attracted attention as a potential source of valuable bioproducts [6].

A significant drawback of cellulose in biomedical applications [7] is its solubility in water and common solvents, caused by the stabilization of intra- and intermolecular hydrogen bonds and electrostatic and hydrophobic interactions within the fibrils [8]. Nanocellulose derived from cellulose have many applications, due to its nano dimensions, a larger surface area and a unique identity, making it an exciting material to research. These smaller dimensions are achieved by removing the amorphous phase of cellulose particles [9].

Thus, keeping in mind about these facts, this study intends to prepare nanocellulose from neem sawdust using ionic liquid (1-butyl-3-methylimidazolium chloride). The FT-IR, XRD, SEM and thermogravimetric analysis were utilized to examine the effects of ionic liquid treatment on the dissolution, morphology, thermal stability, crystallinity and size of the nanocellulosic materials.

EXPERIMENTAL

The neem sawdust was collected from a local sawmill in Davanagere, India. Sodium chlorite, sodium hypochlorite, acetic acid, sodium hydroxide, 1-methylimidazole, chlorobutane and 1-butyl-3-methylimidazolium chloride were purchased from Loba Chemie Pvt. Ltd. All chemicals have a purity of ≥ 98% and the double distilled water was prepared on a lab scale.

Isolation of cellulose from neem sawdust: The isolation of cellulose from neem sawdust was done by two processes *viz*. delignification and decolourization also known as bleaching [10]. The neem sawdust (20 g) and 10% of NaOH were heated for 2 h in the delignification step [11]. The mixture so obtained was washed several times with purified water until the soapy nature of NaOH was not observed [10]. The residue was then collected and dried on a glass petri plate, sieved and weighed [12].

In the decolorization step, the delignified sample was placed in a round-bottom flask followed by the addition of 5% sodium chlorite solution. The mixture was boiled for 1 h, and then 5 mL of sodium hypochlorite was added. The gradual addition of 10 mL of glacial acetic acid during 1 h of heating results in the formation of a white cellulose precipitate. The mixture was further subjected to multiple decantations to collect the white residue. The obtained residue was then transferred to a Petri plate for drying cellulose [13]. Finally, the dried cellulose is weighed and collected.

Synthesis of nanocellulose using ionic liquid: To a clean, dried two-necked round bottom flask, added 30 mL of ionic liquid and place in an oil bath maintaining a range of 120-122 ºC. The cellulose was added gradually to avoid agglomeration with continuous stirring and the mixture was allowed to react for 1 h until the pale yellow solution was visible [14]. The reaction was quenched by adding cold distilled water to the flask, resulting in the formation of precipitate. The precipitate was washed with distilled water 5-8 times to obtain high grade nanofibers. The nanocellulose was dried and transferred into a clean container for further use .

Characterization: The infrared spectra of different materials were captured using Bruker ATR alpha instrument at 25.0 ± 0.5 ºC in the 4000-400 cm^{-1} range to identify various functional groups. For examining the crystal nature of a material, the XRD data was recorded by using a Bruker D8 Advance Diffractometer instrument. To investigate the surface morphology of nanocellulose obtained from neem saw dust, the sample was scanned using a Hitachi SU 3500 scanning electron microscope (SEM) operating at an accelerating voltage of 10 kV at different magnifications. Thermogravimetric analysis (TGA) and differential thermal analysis (DTA) were carried out utilizing the Perkin-Elmer STA 6000 instrument.

RESULTS AND DISCUSSION

FTIR studies: The FTIR spectra of neem cellulose, commercial cellulose and nanocellulose are shown in Fig. 1. Several common absorption peaks associated with cellulose samples were observed at 3343 cm^{-1} showing strong hydrogen-bonded O-H stretching. The peak at 2900 cm^{-1} represents the C-H stretching, the band at 1633 cm^{-1} shows the C=C stretching vibration of acetyl and uronic ester groups; the another peak at 1318 cm^{-1} shows the characteristic C-O stretching and 896 cm^{-1} reveals the presence of β-glycosidic linkage. The spectra confirmed the presence of preserved cellulose structure due to the appearance of the same characteristic peaks from all three samples. The C-H and O-H stretching in commercial cellulose and neem cellulose likely show stronger intensity when compared to prepared nanocellulose. Nanocellulose could have varied the interactions of O-H groups leading to decreased H-bonding within the nanostructure by ionic liquid treatment. The presence of a C=C stretch conjugated group indicates that nanocellulose has a different amount of unsaturation when compared to commercial cellulose. The C-O stretching intensity was higher in nanocellulose is a key feature of cellulose suggesting structural modifications due to size reduction. The β-glycosidic linkage peak is more pronounced in each sample resulting from the breakdown of hydrogen bonding and increased surface area of the nanoscale. It is a backbone and fundamental structure of cellulose which remains intact in nanocellulose when processed with ionic liquid treatment indicating that β-glycosidic bonds are secured during the processing of nanocellulose even when the material undergoes size reduction leading to more surface area and a higher degree of functional groups. Overall,

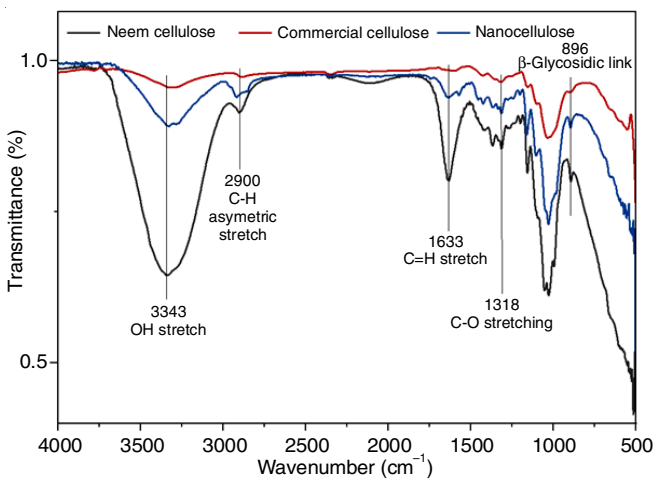

Fig. 1. FTIR of neem cellulose, commercial cellulose and nanocellulose

the FTIR results emphasize the effect of treatment on cellulose structure offering important information for potential applications.

SEM: The SEM images highlight the surface morphology and dimensions at different magnifications. A semicircular, unorganized, inconsistent network is observed in the prepared nanocellulose from neem sawdust with the size range of 198-496 nm (Fig. 2). At higher magnification, the image provides in detailed fibrous structure of nanocellulose, which is a characteristic feature of nanocellulose. It represents a dense agglomeration of entangled fibrils with the typical size range from micro to nanoscale, as the fibers are several microns in length, different shapes of fibers having nonuniform and rough surfaces, irregular cross sections and lumen along with more number of tiny microfibrils. At lower magnification, it exhibits a broader view of nanocellulose structure, which contains complex fibrils with more dispersed as compared in the higher magnification image. The fibrils of nanocellulose show the heterogeneous nature of the material, which is expected in the nanocellulose.

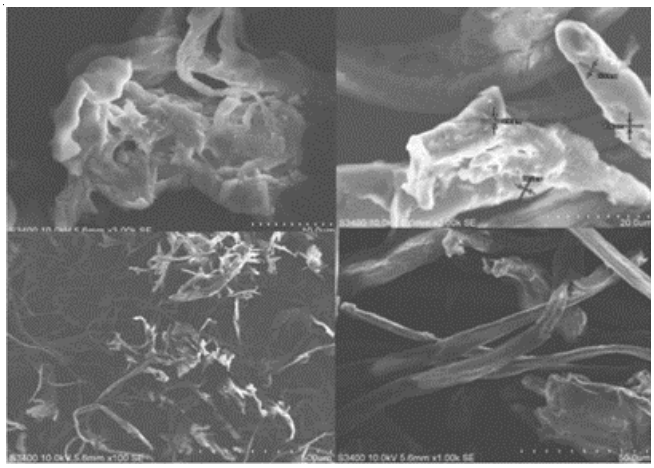

Fig. 2. SEM of neem nanocellulose

Thermal studies: Thermogravimetric and differential thermal analysis curves of dried nanocellulose are shown in Fig. 3. TGA analysis was conducted at a heating rate of 10 ºC/min. At 262.6 ºC, the thermal degradation begins due to the mass loss and reaches a midpoint at 314.9 ºC, therefore suggesting a significant decomposition. This deterioration process continues until the temperature hits around 365.9 °C, at which the overall mass loss reaches about 96.45%, according to the TG analysis. This significant mass loss indicates that the nanocellulose is volatilizing or nearly completely disintegrating, as most of its components are become volatile. The reason is attributed to the the breakdown of nanocellulose particularly the glycosidic linkage breakdown and release of volatile compounds. Concurrently, the DTA curve reveals an exothermic peak at 348.8 ºC, which represents a clear correlation between mass loss and thermal energy release as the peak is located at the middle of the mass loss as observed in the TGA plot. This exothermic property indicates that the energy is being released by the sample during this thermal event, which is connected

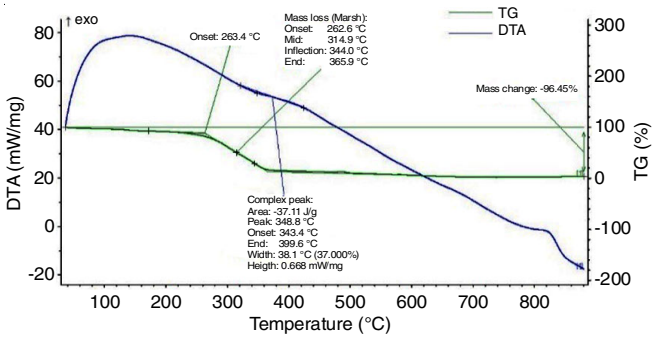

Fig. 3. TGA and DTA of neem nanocellulose

to phase transitions or breakdown events taking place inside the nanocellulose. This thermal event begins at 343.4 ºC, with a maximum peak of 348.8 ºC, which indicates the breakdown of glycosidic linkage was observed and ends at 399.6 ºC, with the height of the exothermic peak being 0.668 mW/mg, as it reflects the thermal process. The combined data indicates that the nanocellulose possesses a significant thermal degradation event within the temperature range, along with the release of heat.

XRD studies: The XRD pattern of nanocellulose reveals several peaks, including 14.5º and 19.8º, which are associated with the 110 and 200 planes of native cellulose as they are separated from 120º indicating that the ionic liquid process has not fully disrupted the crystalline regions of cellulose. The strongest peak at 22.5º [15,16] is the 002 plane and reflects the crystalline nature of cellulose fibers which indicates that there is interlayer spacing between them. Another peak at 28.6º may indicate a change or new crystalline structure formed due to ionic liquid, small amounts of amorphous content or different crystalline structures not typically observed in unmodified cellulose. The remaining peaks at 29.2º, 30.9º, 41.6º and 51.8º suggest the presence of other crystalline phases or impurities, possibly due to the formation of carboxylate groups ionic liquid method in cellulose (Fig. 4). The overall XRD pattern indicates that the ionic liquid method of nanocellulose maintains a substantial level of crystalline structure, specifically, the cellulose I phase, with the presence of additional peaks that are likely attributed to newly formed crystalline phases or oxidation by-

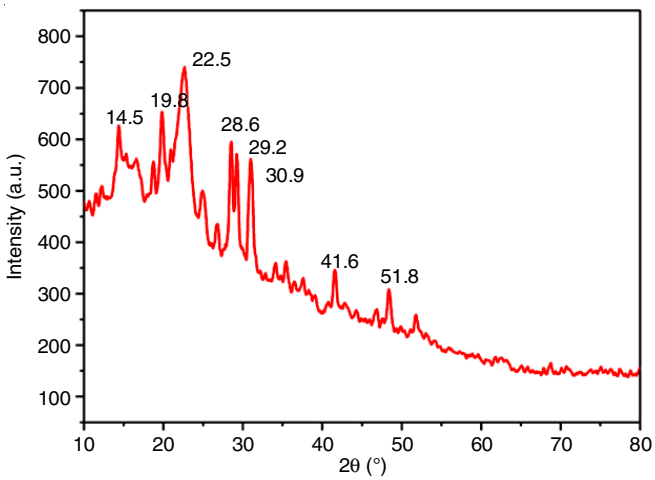

Fig. 4. XRD spectrum of ionic liquid processed nanocellulose

products. The presence of well-defined peaks suggests a significant level of crystallinity, which the oxidation process may have further improved.

Conclusion

The nanocellulose was successfully synthesized from neem sawdust as biomass using ionic liquid and characterized by FTIR, SEM, XRD and TGA/DTA techniques. By utilizing ionic liquid, cellulose dissolves effectively and regenerates nanocellulose. The FTIR results confirmed the presence of β-glycosidic linkage, which is present in all the three samples (nanocellulose, cellulose and commercial cellulose). The SEM results revealed that the nanocellulose is fibrous with dense agglomeration and contains fibers of several microns in length having nonuniform surfaces. It also exhibits a heterogeneous nature of material in nanocellulose of varying dimensions and flexibility with strong fibers. The TGA/DTA analysis shows that nanocellulose exhibits limited thermal stability, as within a specific temperature range, it undergoes significant mass loss and decomposition. The XRD confirmed that the synthesized nanocellulose possesses a high degree of crystallinity with a prominent cellulose I phase, representing its potential suitability for applications required for the structural stability of nanocellulose. These results suggest that the ionic liquid method was an effective process for developing exquisite nanocellulose.

CONFLICT OF INTEREST

The authors declare that there is no conflict of interests regarding the publication of this article.

REFERENCES

1. A. Blasi, A. Verardi, C.G. Lopresto, S. Siciliano and P. Sangiorgio, *Recycling*, **8**, 61 (2023); https://doi.org/10.3390/recycling8040061
2. M. Mujtaba, L. Fernandes Fraceto, M. Fazeli, S. Mukherjee, S.M. Savassa, G. Araujo de Medeiros, A. do Espírito Santo Pereira, S.D. Mancini, J. Lipponen and F. Vilaplana, *J. Clean. Prod.*, **402**, 136815 (2023); https://doi.org/10.1016/j.jclepro.2023.136815
3. U. Udokpoh and C. Nnaji, *Recent Progr. Mater.*, **5**, 6 (2023); https://doi.org/10.21926/rpm.2301006
4. P.H. Keshavamurthysetty and D.H. Patel, *Adv. Nat. Sci. Nanosci. Nanotechnol.*, **15**, 045012 (2024); https://doi.org/10.1088/2043-6262/ad7c1a
5. D. Tavares, M. Cavali, V de OA. Tanobe, L.A.Z. Torres, A.S. Rozendo, A. Zandoná Filho, C.R. Soccol and A.L. Woiciechowski, *Biomass*, **2**, 195 (2022); https://doi.org/10.3390/biomass2030013
6. J.H. Kim, B.S. Shim, H.S. Kim, Y.J. Lee, S.K. Min, D. Jang, Z. Abas and J. Kim, *Int. J. Precis. Eng. Manuf. - Green Technol.*, **2**, 197 (2015); https://doi.org/10.1007/s40684-015-0024-9
7. H.K. Pradeep, D.H. Patel, H.S. Onkarappa, C.C. Pratiksha and G.D. Prasanna, *Int. J. Biol. Macromol.*, **207**, 1038 (2022); https://doi.org/10.1016/j.ijbiomac.2022.03.171
8. H. Seddiqi, E. Oliaei, H. Honarkar, J. Jin, L.C. Geonzon, R.G. Bacabac and J. Klein-Nulend, *Cellulose*, **28**, 1893 (2021); https://doi.org/10.1007/s10570-020-03674-w
9. A.A. Shamsuri, S.N.A. Md. Jamil and K. Abdan, *Front. Mater.*, **9**, 919918 (2022); https://doi.org/10.3389/fmats.2022.919918
10. A.P. Travalini, E. Prestes, L.A. Pinheiro and I.M. Demiate, *J. Polym. Environ.*, **26**, 789 (2018); https://doi.org/10.1007/s10924-017-0983-8
11. Y. Yue, J. Han, G. Han, G.M. Aita and Q. Wu, *Ind. Crops Prod.*, **76**, 355 (2015); https://doi.org/10.1016/j.indcrop.2015.07.006
12. P. Chuayplod and D. Aht-Ong, *J. Met. Mater. Miner.*, **28**, 106 (2018); https://doi.org/10.14456/jmmm.2018.33
13. R. Andalia, R. Rahmi, J. Julinawati and H. Helwati, *J. Nat.*, **20**, 6 (2020); https://doi.org/10.24815/jn.v20i1.12016
14. H.S. Onkarappa, G.K. Prakash, G.H. Pujar, C.R. Rajith Kumar, Radha, M.S. Latha and V.S. Betageri, *Adv. Nat. Sci. Nanosci. Nanotechnol.*, **11**, 035001 (2020); https://doi.org/10.1088/2043-6254/ab9d23
15. H.K. Pradeep and D.H. Patel, *Asian J. Chem.*, **36**, 2079 (2024); https://doi.org/10.14233/ajchem.2024.32127
16. P.H. Keshavamurthysetty and D.H. Patel, *Indian J. Pharm. Educ. Res.*, **57(1s)**, s32 (2023); https://doi.org/10.5530/ijper.57.1s.5